Experimental investigation of nitric oxide radiation in the shock-heated air

P V Kozlov

Institute of Mechanics Lomonosov Moscow State University, Moscow, Russia

E-mail: kalevala@mail.ru

Abstract. The experimental results of the absolute measurements of spectral radiation of air were obtained on the double diaphragm shock tube of Laboratory of Kinetic Process in Gases of Institute of Mechanics MSU. The radiative properties of nitric oxide in the spectral range 190-290 nm were investigated experimentally. The time dependence of the emission of molecular bands for NO shock wave velocities of 4-10 km / s were obtained. The article discusses the problems of absolute power measurement in the radiation behind shock wave front

1. Introduction

Estimation of effects of thermal and radiation fluxes on the aerospace vehicle surface in N_2–O_2 and CO_2–N_2 media during the aerocapture is currently of interest in connection with projects of mission to Earth, Mars and Venus. Up to now, some shock tube measurements of radiation intensities were carried out as a test data for validation the chemical kinetic models describing Earth, Mars and Venus atmosphere entry processes in [1]–[6].

Usually the optical designs of spectrographs are optimized to enable spatially resolved imaging over the length of the instrument's entrance slit. Spatial resolution is maintained at the exit plane, by this means providing dispersed spectra at multiple points simultaneously. The spectrally and spatially resolved image at the exit plane is recorded by an ICCD – at a short exposure time of 0,1–1 ms. Known as imaging spectroscopy, the technique has been implemented in the shock tube experiment in NASA Ames Research Center, University of Queensland and Chofu Aerospace Center [7]–[9]. This method has great potential in the study of radiative processes in shock waves. However, it features some difficulties, such as the deviation of intensity linearity from exposure time [7]. Also, if the length of the nonequilibrium radiation is less than the duration of the exposure of the ICCD, the investigation of nonequilibrium kinetics of radiation on the shock wave is virtually impossible. It is necessary to introduce a so-called non-equilibrium metric [10]. This is equivalent to the integration mode of the CCD measuring the shock wave radiation in the cross-section, as in our experiments.

In the present experiments, the duration of nonequilibrium radiation is in the range of hundreds of nanoseconds. Therefore, the use of the measuring channel, which registers the radiation of the shock wave through the PMT, provides additional information on the kinetic processes in the nonequilibrium zone. This type of data cannot be received for imaging spectroscopy in shock tubes experiments.

This paper represents description of a two-diaphragm shock tube and the results of measuring the absolute intensity of radiation of air heated in the shock waves with velocities V_{SW}=4–10 km/s.

2. Experimental Setup

Experimental investigations carried out in the double diaphragm shock tube (DDST) facility located at the Institute of Mechanics of Moscow State University. Schematic diagram of DDST given in figure 1. Inner diameter of all three seamless tube chambers is equal to 50 mm. Shock tube sections are provided with gateways for P1-P10 piezoelectric sensor mounting allowing to perform control of gas pressure and velocity of shock wave in each section. Transducer signal registered by 14–bit oscilloscope with 10MSa/s sample rate.

Burning mixture of $0.5(H_2+½O_2)+0.5He$ was used in the high-pressure chamber (HPC). The high-pressure chamber operated in the detonation-driven regime. The preparation of mixture produced in HPC. Hydrogen added to the preliminarily prepared mixture of helium and oxygen. HPC operational stability in the detonation regime substantially depends on duration of mixing of the burning gases. To ignite the mixture automobile spark plug used in the rear edge of the HPC. The discharge in the utilized spark plug appeared because of self-breakdown. The stored electrical energy on the high-voltage energy discharge capacitors did not exceed 100 mJ, the duration of discharge was approximately 300÷400 ns. Nanosecond discharge times are achieved by construction of the capacitors and spark gap forming a low-inductance circuit. To achieve rapid shaping of the plane front of combustion in the burning mixture the prechamber was arranged between the rear flange holding the spark plug and the section HPC. HPC filled by mixture $0.5(H_2+½O_2)+0.5He$ up to the total pressure of 400÷600 kPa.

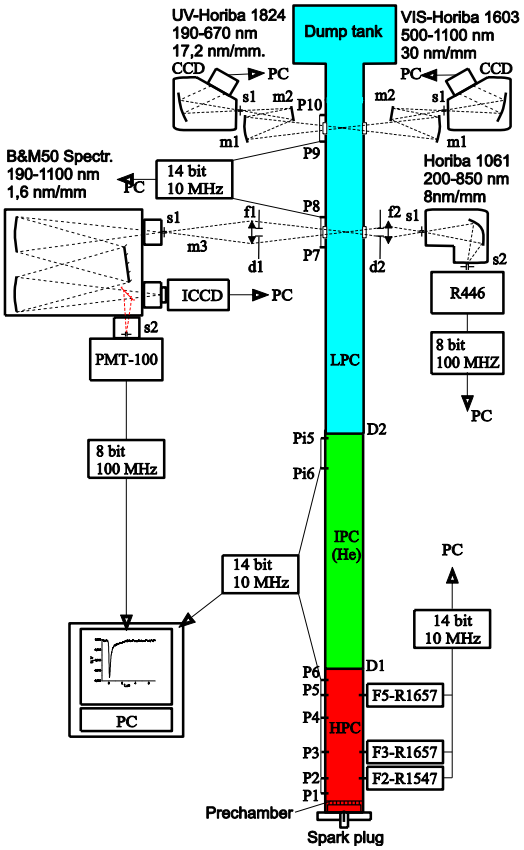

Figure 1. Experimental setup. Shock tube and system of registration.

Initial pressure of air P_1=25÷133 Pa in low pressure chamber (LPC). Changing the pressure and the gas composition (pure helium or a mixture of helium and neon) in the intermediary pressure chamber (IPC), it allows you to get a shock wave speed of 4÷10 km / s. Note that the use of the intermediate chamber with helium eliminates radiation from the contact area for all the shock wave velocity. Reproducibility of the operating parameters of the shock tube, from run to run are about 2% and

basically determined by a quality of the mixture in HPC and a copper thickness of the diaphragm. Dump tank volume of 40 liters and LPC of shock tube evacuated up to 10^{-3} Pa by means of the dry pumping system with a leakage lower than 0.001 Pa/min (likely speed of degassing). To prepare the mixture of sample gas used pure gases produced by AGA Company. In the test experiments, the air gas fills up from the surrounding atmosphere in the low-pressure chamber. In this case, amount of water vapor and carbon dioxide was not controlled. Some works [11], [12] have shown a significant effect of driver gas on physicochemical processes in the driven shock-heated gas. This is because the diaphragm rupture occurs in finite time. The influence of driver gas diminished by means of intermediate section filled by helium. The pressure of helium in the buffer section was 10 kPa. Our work [13] describes in more details effects of driver gas on driven gas in a conventional shock tube operating in one and two diaphragm modes.

3. System Registration

Consider some parameters of optical registration system. Calibration of measured signal values to the absolute spectral radiance ($W/cm^2/\mu m/sr$) was executed with utilization of tungsten (SI−10) and deuterium (DDS−30) lamps calibrated by VNIIOFI. More detailed description of calibration procedure is presented in [4]. For better comparison of results obtained at different facilities, shock tube diameter should be considered, thus the experimental results are presented in the form of a spectral power density B_λ ($W/cm^3/\mu m/sr$). The spectral dispersion of the spectrograph with ICCD (ANDOR−520−18F−03) was 0.04 nm/pix. ICCD strobing was initiated by piezoelectric transducer P7. Minimal duration of strobe achieves up to 0.1 μs, and its location respective shock wave front can be determined with at least 0.5 μs accuracy. ICCD spectral sensitivity area is within 170÷850 nm. Measurements were carried out within 190÷850 nm. Spectrograph with ICCD allowed probing 25 nm of spectrum with high spectral resolution. Emission from the same direction as for the ICCD may be goes by mirror on PMT100 for investigation of temporal behavior of signal in spectral region 190÷850 nm. With splitter m3 the part of the radiation of the shock wave is directed to the spectrograph operating in the spectral range of 190-700 nm with PMT 100. Photomultiplier signal was registered by digital oscilloscope (8-bit, 100 MHz bandwidth). Temporal resolution of this scheme was 0.02 μs and was basically determined by the geometry of optical scheme. This PMT not calibrated in absolute units.

There is a radiation detection channel using photomultiplier R446 Hamamatsu. The photomultiplier is set at the output of the spectrograph Horiba−1061. The width of the recorded spectrum is 4 nm, and the temporary channel resolution of at least 0,04 μs. This PMT calibrated in absolute units in the spectral range 190÷800 nm. There are two channels that detect radiation in the spectral range of 190÷670 nm (UV) spectrograph Horiba CP140-1824 and range of 500÷1100 nm (VIS) spectrograph Horiba CP140-1603. The output spectrographs mounted gated CCD line Hamamatsu S11156. Both channels are calibrated in absolute intensity units. All channels (CCD and ICCD) that detect the spectral intensity distribution given the integral value during the emission across a shock wave passing by the measuring section. The integration time for the absolute values of the spectral distribution determined from the experimental temporary distribution of the radiation. Experimental procedure for measuring the intensity of the radiation emitted by the shock wave is given in [4].

4. Results of Experiment

Figure 2 shows the spectral distribution obtained with high spectral resolution on the ICCD camera in the experiment and the spectral distribution of γ,δ,β,ε-bands nitric oxide calculated for equilibrium conditions at a temperature of 6000K. In the spectral region from 400 nm to 1100 nm are observed primarily atomic oxygen and nitrogen lines.

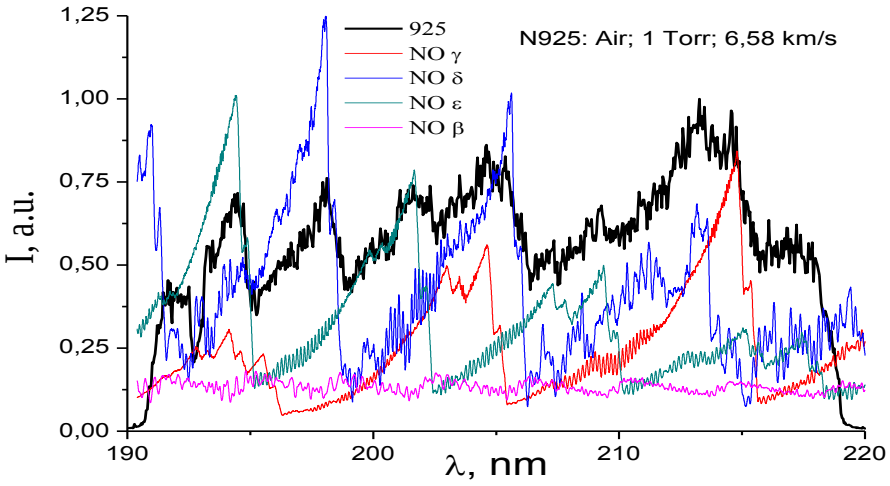

Figure 2. Spectral distribution of integral on time emissivity of air heated by shock wave (P_1=1 Torr, V_{SW}=6,58 km/s) and spectral distribution of γ,δ,β,ε-bands nitric oxide calculated for equilibrium conditions at a temperature of 6000K.

Temporal distributions of the intensities and spectral radiance for 10.4 km/s speed of the shock wave are presented in figure 3, 4. In the spectrum identified molecular nitrogen (the second positive system), nitrogen ion (the first negative system), nitric oxide (δ, γ , ε systems) and CN (violet band system) Observed carbon and hydrogen lines and CN violet bands in the spectra associated with the presence of impurities in the test air. As shown in [14] carbon impurity concentration of 1% in the test air contributes to the radiation from the violet CN bands compatible with of the radiating of N_2^+(B) and N_2(C) in the wavelength range from 290÷480 nm.

The integration of the experimental spectra recorded with a CCD camera was determined from the condition of the shock core length of 10 cm.

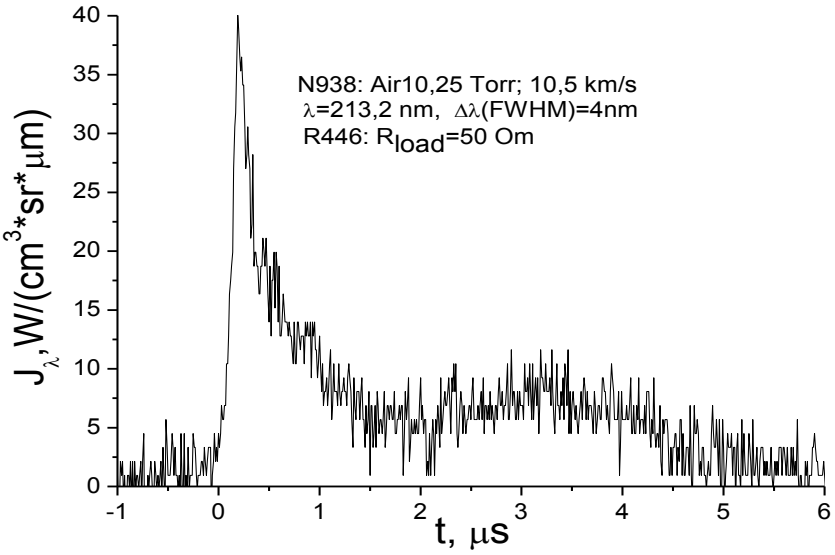

Figure 3. Experimental volumetric radiance profiles of air heated by shock wave P_1=0,25 Torr, V_{SW}=10,4 km/s.

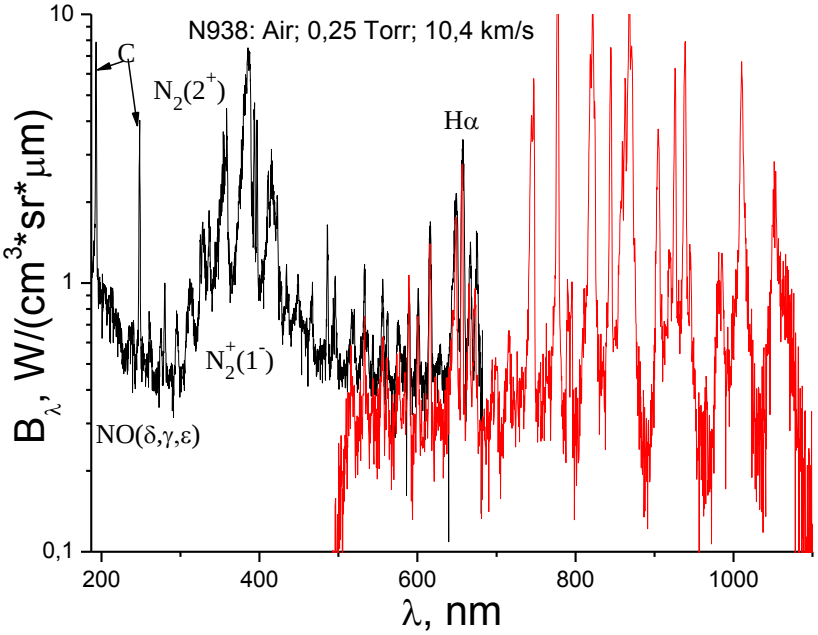

Figure 4. Spectral distribution of integral on time emissivity of air heated by shock wave P_1=0,25 Torr, V_{SW}=10,4 km/s.

Figures 5 ,7, 9, 11, 13 show examples of the volumetric radiance profiles of the nitric oxide emission obtained experimentally on PMT R446. The volumetric radiance profiles from PMT 100 in figure 13 obtained by conversion from the spectral distribution of emissivity with figure 14. The spectral distribution of integral on time emissivity in the wavelength range 190÷450 nm, recorded with a CCD camera shown in figures 6, 8, 10, 12, 14.

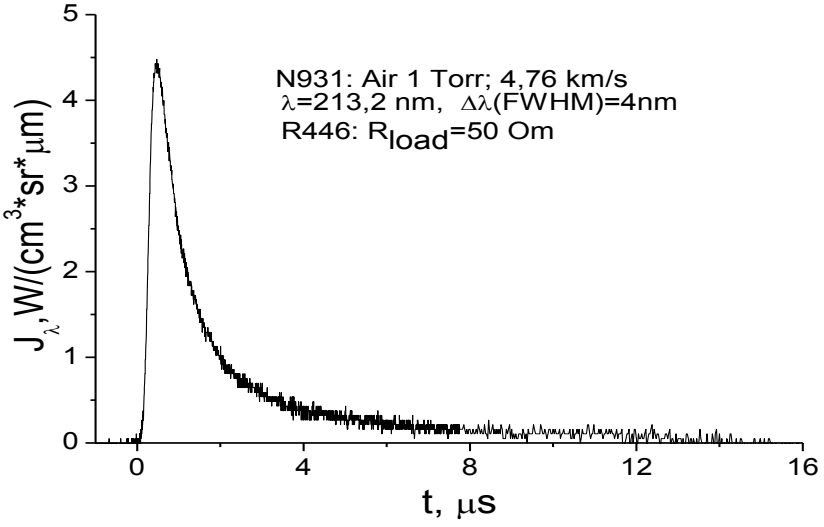

Figure 5. Experimental volumetric radiance profiles of air heated by shock wave P_1=1 Torr, V_{SW}=4,76 km/s.

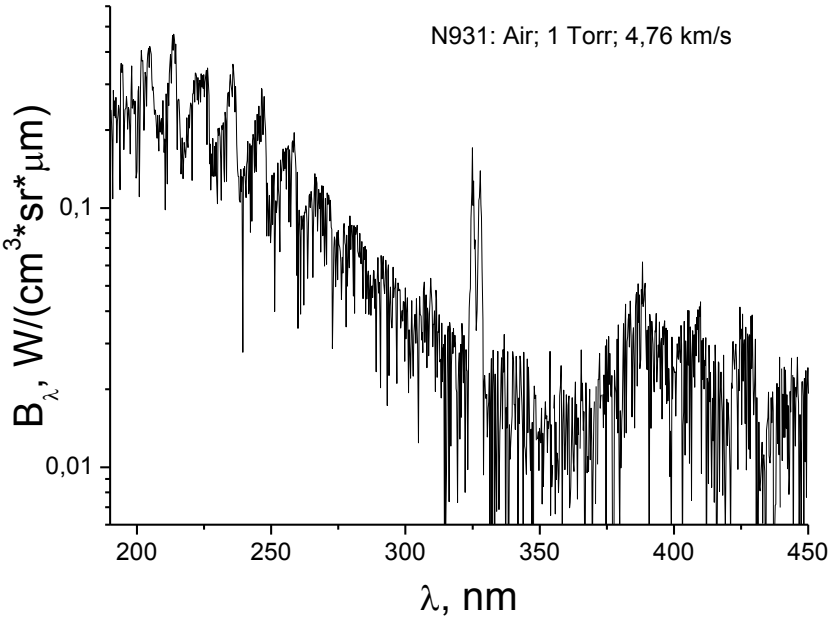

Figure 6. Spectral distribution of integral on time emissivity of air heated by shock wave P_1=1 Torr, V_{SW}=4.76 km/s.

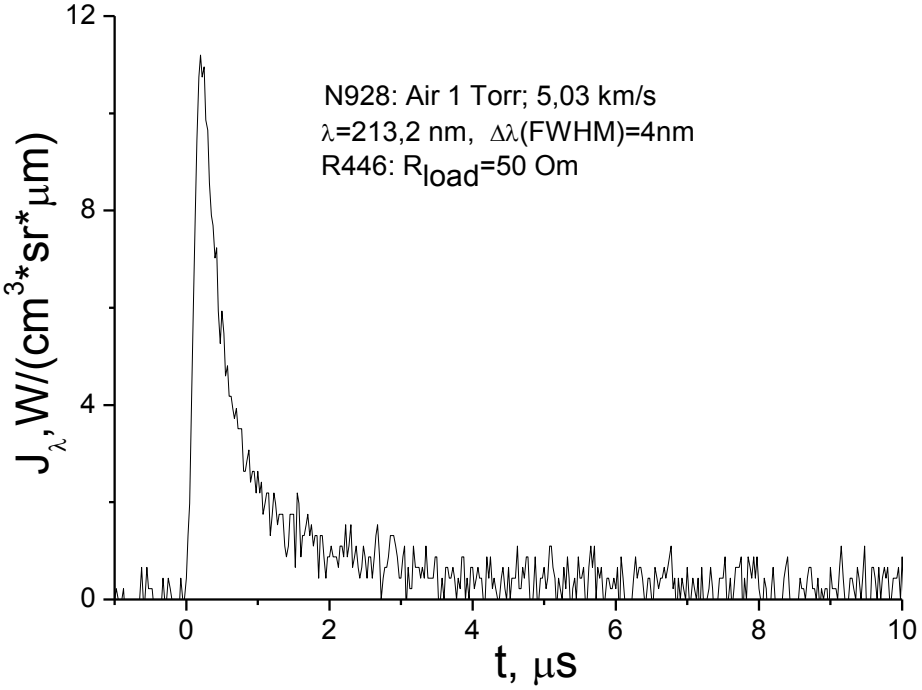

Figure 7. Experimental volumetric radiance profiles of air heated by shock wave P_1=1 Torr, V_{SW}=5.03 km/s.

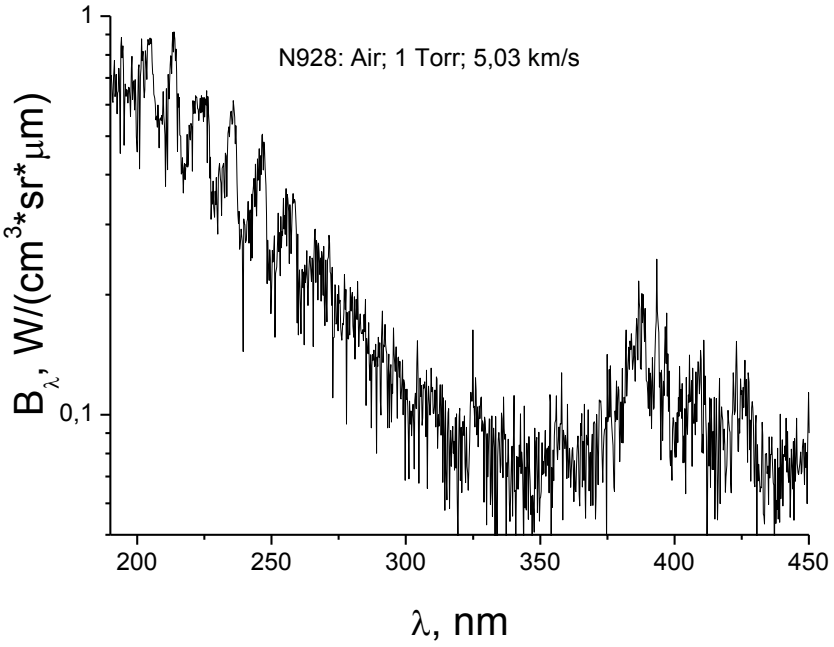

Figure 8. Spectral distribution of integral on time emissivity of air heated by shock wave P_1=1 Torr, V_{SW}=5.03 km/s.

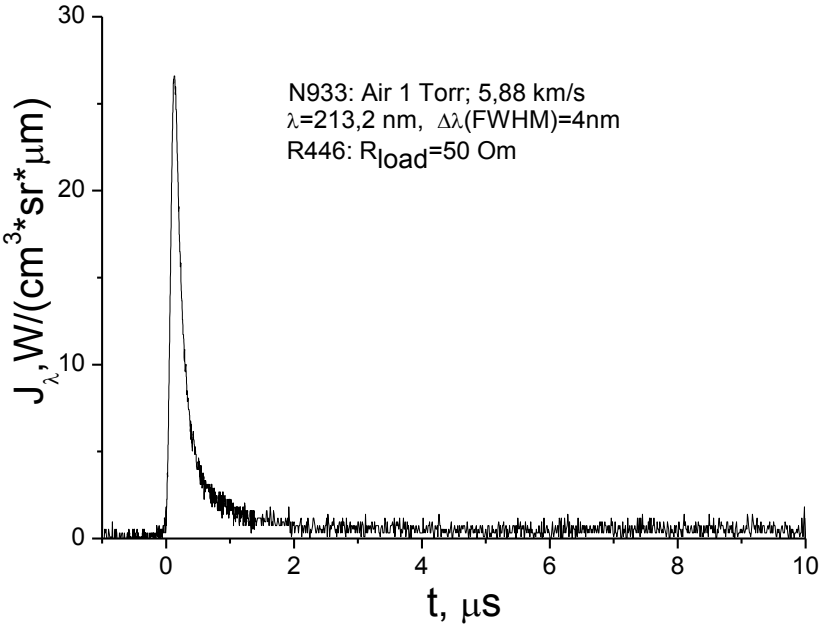

Figure 9. Experimental volumetric radiance profiles of air heated by shock wave P_1=1 Torr, V_{SW}=5.88 km/s.

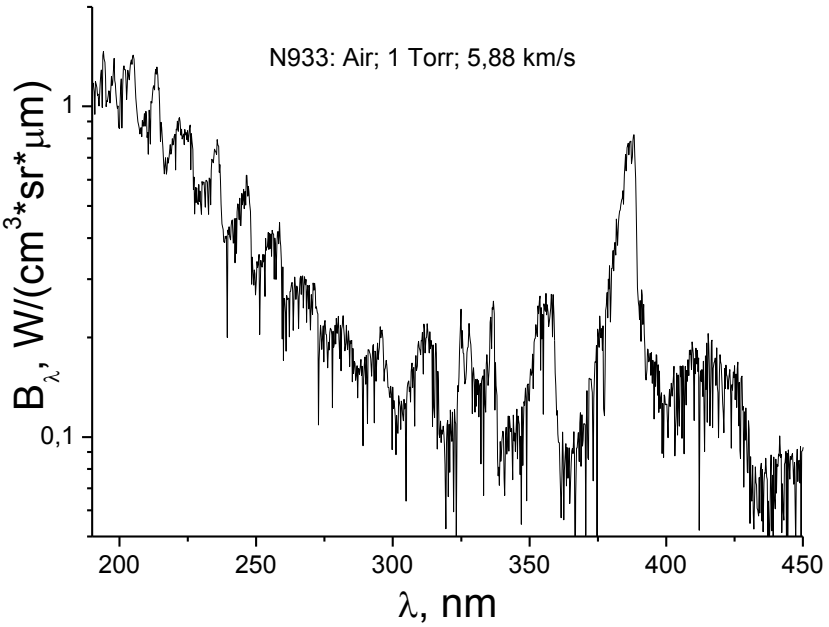

Figure 10. Spectral distribution of integral on time emissivity of air heated by shock wave P_1=1 Torr, V_{SW}=5.88 km/s.

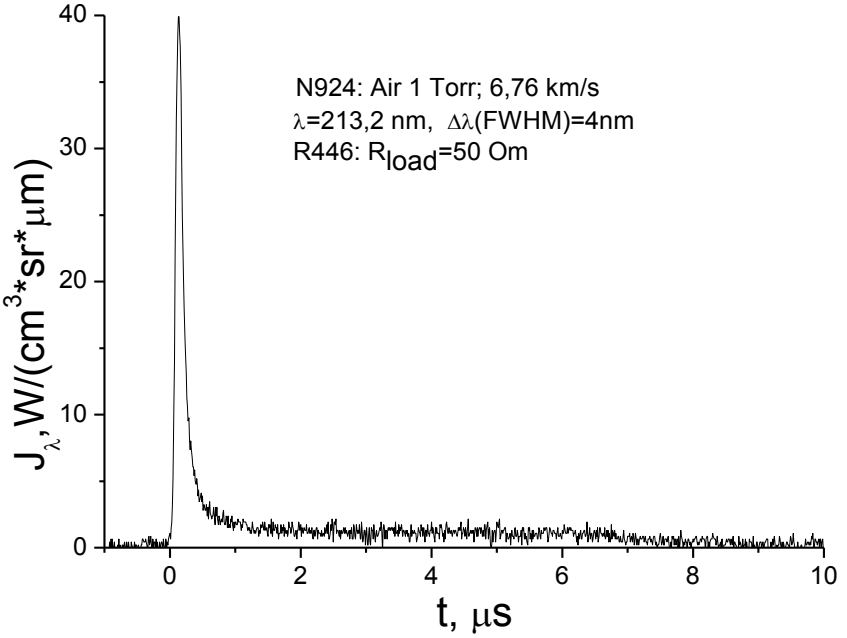

Figure 11. Experimental volumetric radiance profiles of air heated by shock wave P_1=1 Torr, V_{SW}=6.76 km/s.

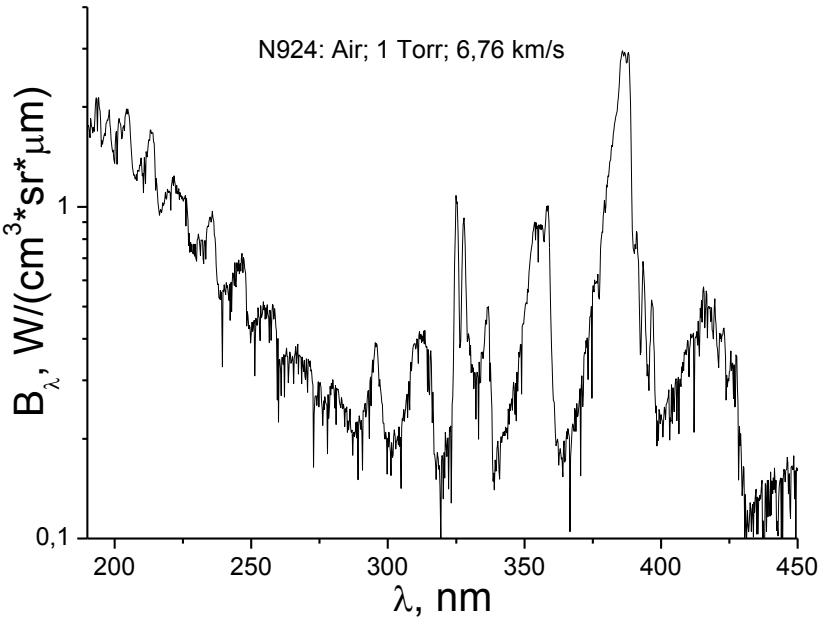

Figure 12. Spectral distribution of integral on time emissivity of air heated by shock wave P_1=1 Torr, V_{SW}=6.76 km/s.

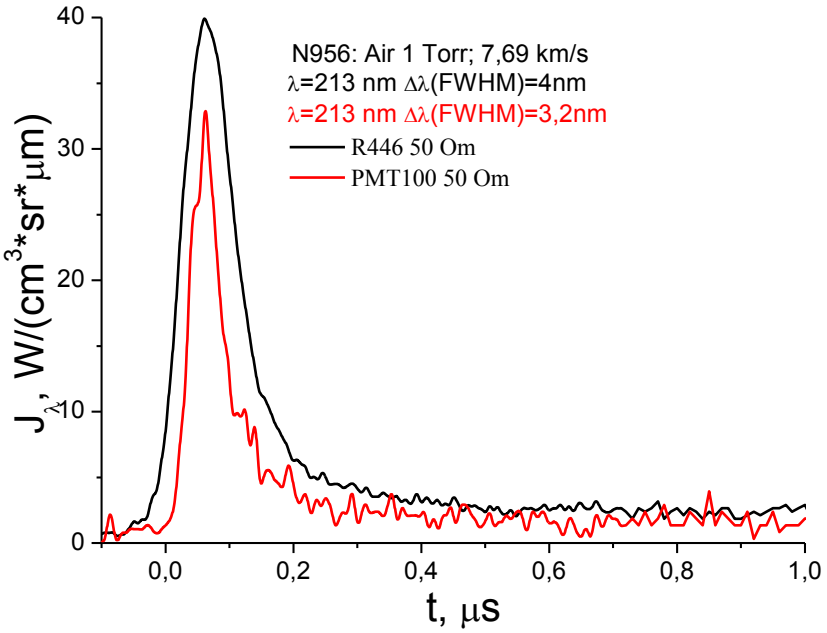

Figure 13. Experimental volumetric radiance profiles of air heated by shock wave P_1=1 Torr, V_{SW}=7.69 km/s.

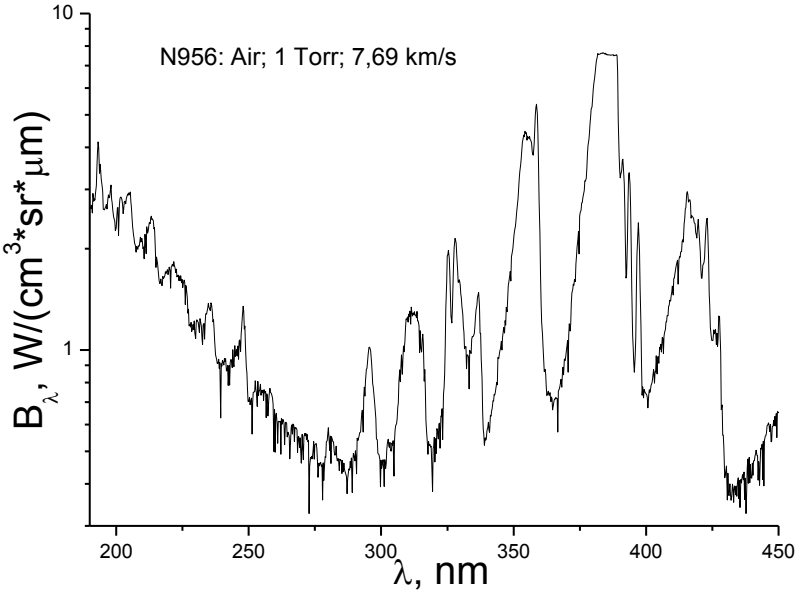

Figure 14. Spectral distribution of integral on time emissivity of air heated by shock wave P_1=1 Torr, V_{SW}=7.69 km/s.

Molecular bands (δ, γ, ε) of nitric oxide predominately emit in the UV spectrum with the shock wave velocity of 4-5.5 km/s. Nitrogen bands (the second positive system) and nitrogen ion (the first negative system) appear in the spectra with the increase of the shock wave speed. Also, atomic nitrogen and oxygen lines occur in the visible region of the spectrum.

The radiation peak depends on the speed and the initial pressure. Under the condition of constancy of the shock wave speed, it can be assumed that the radiation peak depends linearly on the pressure behind the wave (or the initial pressure). Duration of nonequilibrium radiation also depends on the speed and the pressure behind the shock wave. Typically, the peak duration leads to constant pressure behind the shock wave. In this study, the duration and the amplitude of the radiation peak is recalculated to the initial pressure of the test gas at P_1=1Torr.

The intensity of the NO bands increases approximately to the same extent as the increase in the shock wave speed, while the duration of the non-equilibrium radiation peak at a wavelength of 213 nm drops sharply. Figure 15 shows the experimental data of the radiation peak J_λ^{max} vs. the V_{SW}. The peak intensity (rhombic points) of RC-model calculated from [15] under our experiment conditions are shown for the comparison. Spectrally averaged radiations peak NO in the shock wave calculated in [16] are in good agreement with the experimental data of Gorelov [3] for shock speeds below 7km/s, but are lower than the experimental data in [3] at higher shock speeds. The radiation peak saturation is observed at speeds higher 7 km/s in our experiments, which is in agreement with [16].

Experimental data of the duration of the nonequilibrium radiation peak vs. speed is presented on the figure 16. The triangular points shows the duration of the nonequilibrium radiation peak at a wavelength of 236±7 nm recalculated for the pressure P_1=1 Torr, which was previously computed in [16] for the initial pressure P1 = 0.1 Torr. The difference between the calculation results of work [16] and our experiments is probably due to incorrect recalculation of peak for the pressure of 0.1 to 1 Torr. The duration of radiation peak of NO at a wavelength of 213 nm and 236 are practically identical. The time of population on FWHM of electronic states of NO molecule calculated within the RC-model [15] are shown in Figure 16 by rhombic points.

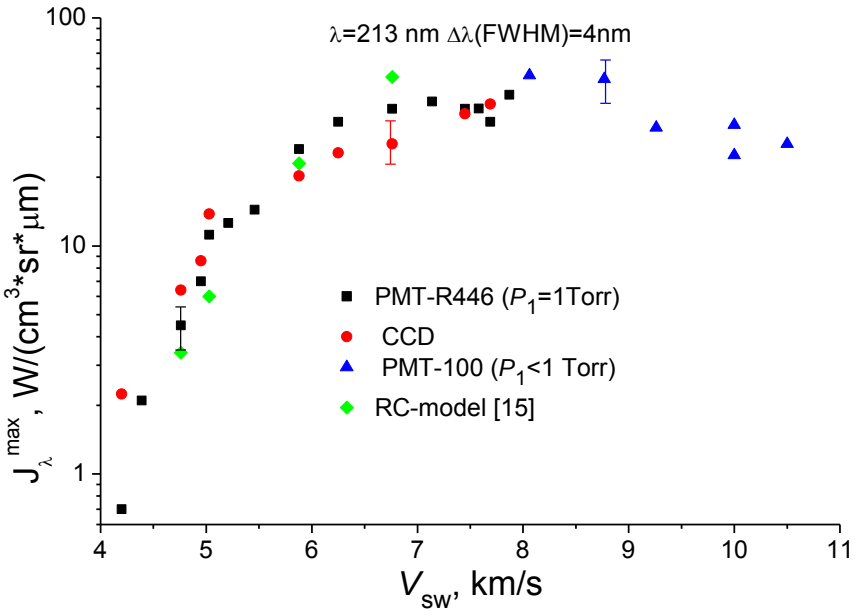

Figure 15. Radiance peak NO (213±2nm) of the shock-wave velocity at P_1=1 Torr.

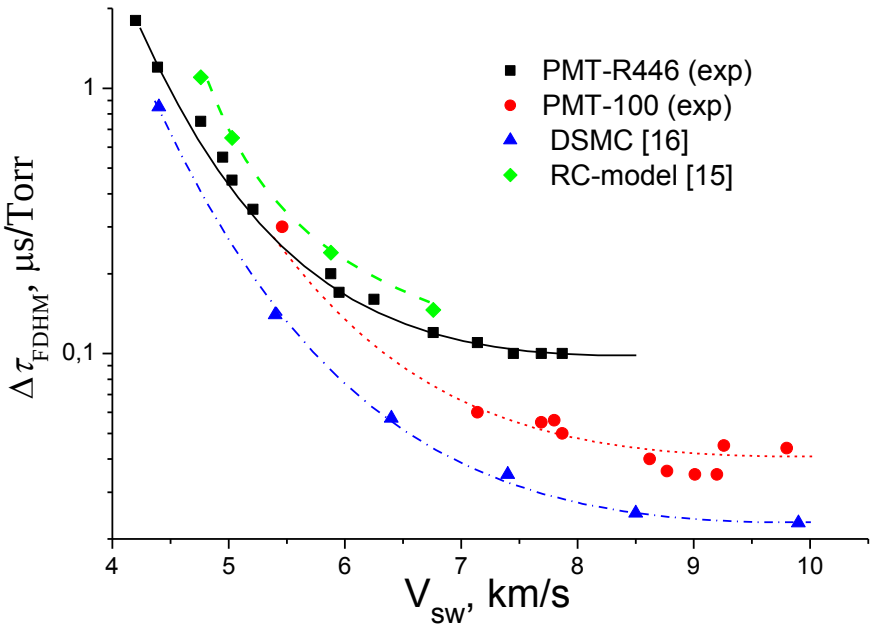

Figure 16 Duration radiance peak (FWHM) of the shock-wave velocity at P_1=1 Torr.

5. Conclusion

Nonequilibrium radiation is a major contributor in the radiation flux received by spacecraft at the entrance to Earth's atmosphere at speeds of 9-11 km / s. The duration of this radiation is very short. The paper shows the possibility of studying nonequilibrium kinetics in shock heated air with high spatial resolution. These experimental data were compared with the results of numerical calculation on the hybrid radiative-collisional model represented in Ref. [15]. Preliminary comparison of experiments described in the article with the results of DSMC simulation presented in Ref. [16] is performed, and proves them to be in a satisfactory agreement.

Acknowledgments

This study was supported by RFBR grant No. 16-01-00379 and by the Program of Basic Researches of Russian Academy of Sciences. The author would like to thank Drs. Shatalov OP and Surzhikov ST for their insight during many fruitful discussions.

References

[1] Dikalyuk A S, Kozlov P V, Romanenko Y V, Shatalov O P and Surzhikov S T 2013 Nonequilibrium spectral radiation behind the shock waves in Martian and Earth atmospheres *44th AIAA Thermophysics Conference AIAA 2013-2505* pp 1– 10

[2] Dikalyuk A S, Kozlov P V, Romanenko Y V, Shatalov and O P Surzhikov S T 2012 Nonequilibrium radiation behind the strong shock waves in Martian and Titan atmospheres: Numerical rebuilding of experimental data *50th AIAA Aerospace Sciences Meeting including the New Horizons Forum and Aerospace Exposition, AIAA* 2012–0795 pp 1–10

[3] Gorelov V A, Gladyshev M K, Kireev A Yu, Yegorov I B, Plastinin Y A and Karabadzhak G G 1998 Experimental and Numerical Study of Nonequilibrium Ultraviolet NO andN_2^+ Emission in Shock Layer *Journal of Thermophysics and Heat Transfer* Vol 12, No 2, pp 172–179

[4] Zalogin G N, Kozlov P V, Kuznetsova L A, Losev S A, Makarov V N, Romanenko Yu V and Surzhikov S T 2001 Radiation Excited by Shock Waves in a CO_2-N_2-Ar Mixture: Experiment and Theory*Technical Physics*, Vol 46, No 6, pp 654-661

[5] Surzhikov S T. 2012 Radiative-Collisional Models in Non-Equilibrium Aerothemodynamics of Entry Probes *Journal of Heat Transfer* **134** pp 031002-1 – 031002-12

[6] Brandis A M, Johnston C O, Cruden B A, Prabhu D K and Bose D 2012 Validation of High Speed Earth Atmospheric Entry Radiative Heating from 9 5 to 15 5 km/s *AIAA Paper 2012–2865* pp 1–23

[7] Cruden B A 2014 Absolute Radiation Measurements in Earth and Mars Entry Conditions *NATO TR RTO-EN-AVT-218* Von Karman Institute for Fluid Dynamics, Rhodes Saint Genese, Belgium pp 1–40

[8] Jacobs C M, McIntyre T J, Morgan R G, Brandis A M and Laux C O 2015 Radiative Heat Transfer Measurements in Low-Density Titan Atmospheres *Journal of Thermophysics and Heat Transfer* Vol 29 No 4 pp 835-844

[9] Takayanagi H and Fujita K 2012 Absolute Radiation Measurements Behind Strong Shock Wave In Carbon Dioxide Flow for Mars Aerocapture Missions *43rd AIAA Thermophysics Conference, Fluid Dynamics and Co-located Conference*s *AIAA 2012-2744* pp 1-12

[10] Brandis A M, Johnston C O and Cruden B A 2016 Non-equilibrium Radiation for Earth Entry *46th AIAA Thermophysics Conference, AIAA AVIATION Forum AIAA 2016-3690* pp1-19

[11] Kozlov P V, Makarov V N, Pavlov V A and Shatalov O P 2000 Experimental investigation of CO vibrational deactivation in a supersonic cooling gas flow *Shock Waves* Vol 10 pp 191–195

[12] Bogdanoff D W and Park C 2002 Radiative Interaction Between Driver and Driven Gases in an Arc-Driven Shock Tube *Shock Waves* Vol 12 pp 205–214

[13] Kozlov P V and Romanenko Yu V 2009 Experimental Investigation of Shock Heated Air

Radiation on the Double-Diaphragm Shock Tube *in Proceedings of the 3th All-Russian School-Workshop Aerophysics and Physical Mechanics* of *Classical and Quantum Systems* (in Russian) pp 21−29

[14] Johnston C 2008 A Comparison of EAST Shock-Tube Radiation Measurements with a New Air Radiation Model *46th AIAA Aerospace Sciences Meeting and Exhibit, Aerospace Sciences Meetings AIAA 2008-1245* pp 1−22

[15] Kozlov P V and Surzhikov S T Nonequilibrium Radiation NO in Shocked Air (2017) *55th AIAA Aerospace Sciences Meeting, AIAA SciTech Forum AIAA 2017-0157* pp 1−16

[16] Zhu T, Li Z and Levin D A 2014 Modeling of Unsteady Shock Tube Flows Using Direct Simulation Monte Carlo *Journal of Thermophysics and Heat Transfer* Vol 28 No 4, pp 623-634